Journal of Applied Automation Technologies

Research Paper

Adaptive State-Space Kalman Filter Model for Tunnel Deformation Prediction

Hamdan Al-Suwaidi[1, *], Zainab Al-Zaabi[1], Amal Al-Hashimi[2] and Mishaala Al-Tunaiji[2]

[1] College of Computing and Information Technology, Abu Dhabi University, Abu Dhabi, PO Box 59911, United Arab Emirates
[2] College of Engineering, Information Technology Division, University of Sharjah, Sharjah, PO Box 27272, United Arab Emirates
*Corresponding author: hamdan.su@adu.ac.ae

Abstract. Accurately predicting tunnel deformation to ensure construction safety, optimize support, and issue structural risk warnings. When settlement gages, convergence gages, inclinometers, and stress sensors are used for monitoring, phased evolution, measurement noise, and incomplete observations often occur. This article proposes a new adaptive state-space Kalman filter model for predicting tunnel deformation. The model uses displacement, deformation velocity, acceleration, surrounding pressure, and construction phase parameters to illustrate the development of deformation. Using the state-space refinement method, update the state transition matrix and noise covariance based on the most recent monitoring residuals. Finally, the optimized Kalman filter calculates the alarm probability and short-term deformation prediction. Based on experimental analysis, ARIMA, support vector regression, neural networks, standard Kalman filters, and deep sequence models were tested. The tunnel monitoring sequence consists of multiple segments. The new technology reduced the noise observation RMSE to 1.36 mm and improved the early warning recall rate to 93.5%. This paper proposes a tunnel deformation monitoring system prediction method that is easier to use and understand.

Keywords: *Tunnel Monitoring, Deformation Forecasting, Adaptive Kalman Filter, State-Space Refinement, Sensor Sequence, Structural Safety Warning*

Received on 03 January 2023, Accepted on 28 May 2023, Published on 08 June 2023

Introduction

Tunnel deformation monitoring is divided into three stages. Excavation, lining construction, support installation, and long-term operation. The changes in rock mass and structural deformation have been continuously monitored by settlement gages, convergence gages, inclinometers, extensometers, stress sensors, and mobile scanning systems. The monitoring data will be used to evaluate the support effectiveness, identify unstable convergence issues, and adjust construction measures before local deformation leads to safety accidents [1]. Visualization of shield tunnel deformation and convergence research based on deep learning indicate that under operational and construction disturbances, sensor sequences can reveal phased deformation patterns [2]. Sensor data and ground settlement predictions from embedded tunnel foundation monitoring have also demonstrated the reliability of data-driven deformation predictions in engineering risk control [3].

However, the tunnel monitoring sequence model is not accurate. Deformation is influenced by the following factors: the distance to the excavation face, the grade of the surrounding rock, groundwater, the stiffness of the lining, the support time, and the construction load. Measurement sequences typically include time-varying noise, missing observations, abrupt changes, and non-stationary trends. Machine learning methods that can model nonlinear relationships include Gaussian process regression and neural networks, but these methods typically require a large amount of training data and have poor interpretability at the state level [4]. Research on shield tunnel settlement prediction and subway ground deformation indicates that data-driven models are appropriate. However, when monitoring conditions change or data is insufficient, the reliability of the model decreases [5].

https://doi.org/10.64972/jaat.2023v1.293p11e:148-159

Although the Kalman filter has good engineering interpretability, the fixed state transition matrix and constant covariance may not be suitable for changes in excavation disturbances and sensor noise [6].

This paper proposes an adaptive state-space Kalman filter model based on multiple monitoring sensors to predict tunnel deformation. The model's displacement, velocity, acceleration, surrounding pressure, and construction phase variables can be used to determine the micro-deformation state of the model. The state transition matrix and noise covariance are adjusted based on the behavior of recent residuals to accommodate the acceleration caused by excavation and the stability provided by support. Research is underway to improve the accuracy of short-term predictions, reduce the accumulation of errors in the presence of missing or noisy data, and create interpretable tunnel safety monitoring warning probabilities.

Related Work

Sensor Monitoring and Tunnel Deformation Prediction

The tunnel deformation monitoring network has recently added fixed sensors, mobile detection systems, and numerical models. By using mobile monitoring systems, cross-sectional deformation analysis can enhance the spatial perception of shape changes in shield tunnels [7]. Research on tunnel construction monitoring indicates that lining, convergence, and settlement deformations are typically related to the phased paths associated with excavation and support times [8]. Monitoring and settlement methods for composite structures: Research on river-crossing shield tunnels indicates that multiple observation sources are needed to detect local deformations and longitudinal irregularities [9].

Tunnel and geotechnical engineering predictions have utilized a large amount of machine learning. In addition to deformation prediction, automated learning, Gaussian process regression, and neural networks have been used to address ground subsidence and geomechanical parameter estimation issues [10]. Research on long-term settlement prediction and defect detection in tunnels indicates that tunnel risk assessment can be supported using monitoring data [11]. However, the performance of the model is crucially dependent on the quality of the data and the stability of the features. According to deformation analysis based on monitoring and InSAR time series prediction, noise and spatial heterogeneity measurements may distort deformation trends [12]. Therefore, the tunnel deformation prediction model should be able to simultaneously handle sensor uncertainty and maintain the continuity of physical states.

Deep sequence models, such as LSTM and Transformer, can improve time series predictions for structural health monitoring and geotechnical displacement forecasting [13]. Due to the lack of labeled deformation events and the requirement for real-time interpretability, deep models are not always suitable for site-level tunnel monitoring. State space filtering has clear dynamic equations and updates predictions upon receiving new measurements. It is suitable for recursive processing because the system continuously receives short sensor sequences from various parts of the tunnel.

Adaptive Filtering and Sequential State Estimation

In structural health monitoring, the Kalman filter and its nonlinear extensions are used for parameter estimation and deformation prediction. The constrained extended Kalman filter and unscented Kalman filter techniques have been used for identifying structural parameters and state assessment [14]. According to the research, state-space methods are suitable for handling unobserved internal states. According to statistical time series models and infrastructure deformation monitoring, sequence estimation can reduce noise and maintain dynamic response [15].

Since the tunnel shape changes over time, the adaptive filter needs to adjust. Fixed covariance may reduce the uncertainty of the stable process while also reducing the uncertainty of the excavation process. The ensemble Kalman prediction of subway surface deformation indicates that filtering can improve monitoring-based predictions by explicitly considering uncertainty [16]. Recursive correction has also demonstrated that using a Kalman filter to predict landslide deformation can reduce prediction drift [17]. Tunnel monitoring is a state-space refinement method that needs to address missing measurements, residuals, and delayed observations, rather than assuming noise is constant.

https://doi.org/10.64972/jaat.2023v1.293p11e:148-159

Time series forecasting and deep learning provide auxiliary baselines. Long sequence models can simulate nonlinear temporal patterns. Informer, Temporal Fusion Transformer, and other deep prediction studies have proven this point [18]. Research on displacement prediction based on LSTM also provides a reference for nonlinear sequence learning [19]. On the other hand, these models are usually complex to train, and the state covariance is opaque. Using an efficient Kalman filter can create a concise, easy-to-train, and easy-to-interpret tunnel deformation prediction model [20]. In uncertain environments, real-time displacement tracking aids in online structural response estimation [21]. Research on deep damage identification indicates that learned schedules can be used to diagnose infrastructure [22]. Sensor network coverage predictions indicate that reliability monitoring must be considered when performing state estimation [23]. Deep prediction models also predict the sequence of structural loosening well [24]. According to the prediction of the Kalman filter, recursive correction can reduce deformation drift [25]. The general prediction model based on Kalman filtering supports low-latency recursive prediction [26]. The recursive state prediction of the Kalman filter aids in hybrid sequence-state modeling [27]. According to the estimates of the unscented Kalman filter with multiple models, the foundation for adaptive state updating has been improved [28]. The research on extended and unscented Kalman filtering provides useful examples for nonlinear monitoring systems [29]. In addition, the quantification of displacement uncertainty also supports the use of posterior covariance in early warning decision-making [30].

Methodology and Experimental Evaluation Framework

Multi-Source Monitoring Sequence Modeling

Record the settlement, convergence, tilt meter data, surrounding pressure, and construction phase observations of multiple tunnel sections. During active construction, samples are taken every 30 minutes, and during stable operation, samples are taken every 2 hours. To ensure the consistency of state estimation, all sensor channels are aligned by timestamp and normalized based on the statistical data from the training phase.

$$y_t = [s_t, c_t, i_t, p_t, e_t] \tag{Eq.(1)}$$

Here, s_t denotes vault settlement, c_t denotes horizontal convergence, i_t denotes inclination response, p_t denotes surrounding pressure, and e_t denotes construction-stage encoding. This observation vector links measurable deformation and disturbance variables.

The deformation state includes displacement, velocity, acceleration, pressure correction, and residual trend. Compared with using displacement alone, this state design allows the model to represent deformation evolution and its shortterm change rate.

$$x_t = [d_t, v_t, a_t, \psi_t, \rho_t]^T \tag{Eq.(2)}$$

The term d_t is the deformation value to be predicted, v_t and a_t describe deformation speed and acceleration, ψ_t represents pressure correction, and ρ_t stores the residual trend caused by unmodeled disturbance.

Sensor sequences often contain missing values and abnormal spikes. A reliability coefficient is assigned to each observation according to missing ratio, local fluctuation, and sensor status.

$$\omega_t = \sigma(W_\omega q_t + b_\omega) \tag{Eq.(3)}$$

When ω_t is low, the model reduces the influence of the current observation and relies more on state prediction. In the dataset, about 7.8% of samples contain at least one incomplete channel. The aligned and reliability-corrected sequence is then used as the input of the refined Kalman Filter. Figure 1 shows how multi-source monitoring records are converted into state vectors and observation vectors for recursive prediction.

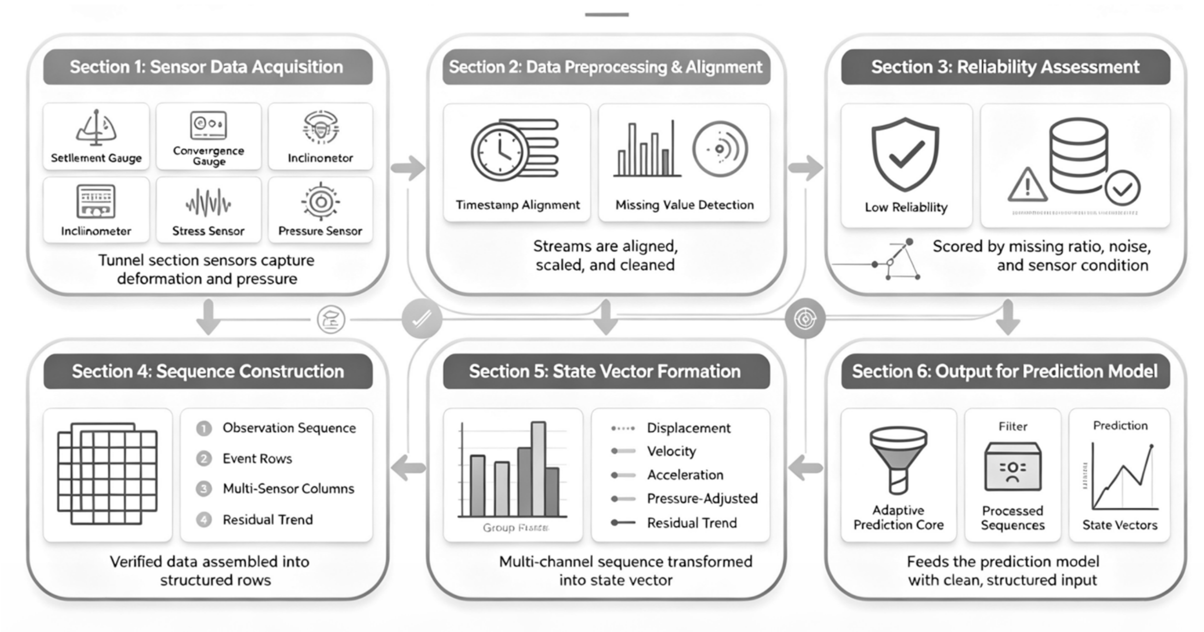

Figure 1. Multi-source tunnel deformation monitoring sequence modeling process

Adaptive State-Space Kalman Prediction Model

The basic state-space model describes the dynamic process of tunnel deformation caused by structural reinforcement and construction disturbances. Due to the different changes in deformation during excavation, support installation, and stable operation, the state transition matrix is not fixed.

$$x_t = F_t x_{t-1} + B_t u_t + w_t \quad \text{Eq.(4)}$$

The control variable u_t contains excavation distance, support timing, and surrounding rock grade encoding. The process noise w_t represents unmodeled geotechnical disturbance.

The observation equation maps hidden deformation state to measured sensor data through H_t, while observation noise r_t is affected by sensor precision, installation condition, and environmental disturbance. During rapid excavation, r_t becomes larger because measurements fluctuate more strongly.

The transition matrix is refined using recent residual statistics. If residuals show persistent positive drift, the deformation acceleration component is strengthened; if residuals decay, the model increases stabilization weight.

$$F_t = F_0 + \lambda_f \frac{e_{t-1} e_{t-1}^T}{\|e_{t-1}\|_2 + \varepsilon} \quad \text{Eq.(5)}$$

Here, e_{t-1} is the previous prediction residual. This residual-driven refinement allows the model to adapt when deformation begins to accelerate before crossing the warning threshold.

The process covariance is also updated by residual energy. High residual energy indicates that the current state transition is uncertain and should be corrected more aggressively.

$$Q_t = \beta Q_{t-1} + (1-\beta) e_{t-1} e_{t-1}^T \quad \text{Eq.(6)}$$

The smoothing coefficient β is set to 0.82. This value avoids abrupt covariance oscillation while preserving sensitivity to excavation disturbance.

Observation covariance is refined according to sensor reliability. Missing or unstable measurements receive larger observation noise, reducing their impact on the posterior state.

$$R_t = R_0 + \lambda_r \mathrm{diag}(1-\omega_t) \quad \text{Eq.(7)}$$

Since a single fault converging instrument should not affect state correction, this update is for the field monitoring section.

In previous predictions, the adjusted transfer and covariance were used. Estimate the deformation before measuring the current value.

$$\hat{x}_{t|t-1} = F_t \hat{x}_{t-1|t-1} + B_t u_t \quad \text{Eq.(8)}$$

The prior covariance propagates uncertainty through the refined state transition.

$$P_{t|t-1} = F_t P_{t-1|t-1} F_t^T + Q_t \quad \text{Eq.(9)}$$

The Kalman gain is calculated from the prior covariance and refined observation covariance.

$$K_t = P_{t|t-1} H_t^T (H_t P_{t|t-1} H_t^T + R_t)^{-1} \quad \text{Eq.(10)}$$

A larger Kalman gain means that the current measurement is reliable and informative. A smaller gain indicates that the filter trusts the predicted deformation state more than the sensor reading.

Training-Free Updating and Evaluation Configuration

The posterior deformation state is updated by combining the prior state and the reliability-calibrated observation residual. The model is training-free in the sense that it does not require backpropagation; only a small group of refinement coefficients is selected on the validation set.

$$\hat{x}_{t|t} = \hat{x}_{t|t-1} + K_t (y_t - H_t \hat{x}_{t|t-1}) \quad \text{Eq.(11)}$$

This recursive update provides an interpretable correction path from measured deformation to hidden state estimation. When measurements are incomplete, the correction term naturally becomes smaller through R_t.

The posterior covariance is updated to quantify remaining uncertainty after measurement assimilation.

$$P_{t|t} = (I - K_t H_t) P_{t|t-1} \quad \text{Eq.(12)}$$

The predicted deformation value is extracted from the first component of the posterior state. A one-step-ahead and three-step-ahead prediction are both generated for early warning.

$$\hat{d}_{t+\tau} = g_d (F_{t+\tau} \hat{x}_{t|t}) \quad \text{Eq.(13)}$$

The function g_d extracts the displacement component from the propagated state. In the experiment, τ is set to 1,3, and 6 monitoring intervals.

The warning probability is calculated from predicted deformation, deformation velocity, and posterior uncertainty. This avoids issuing warnings only after the measured displacement exceeds a threshold.

$$P_w = \sigma\left(\eta_1 \hat{d}_{t+\tau} + \eta_2 \hat{v}_{t+\tau} + \eta_3 \mathrm{tr}(P_{t|t})\right) \quad \text{Eq.(14)}$$

Figure 2 presents the adaptive state-space Kalman prediction workflow. It includes monitoring-sequence alignment, residual-guided state refinement, covariance adaptation, recursive prediction, and warning output.

The evaluation configuration uses chronological splitting to avoid leakage across construction stages. The first 60% of each section sequence is used for initialization and coefficient selection, the next 20% for validation, and the final 20% for testing. The model is compared with ARIMA, SVR, Random Forest, standard Kalman Filter, LSTM, GRU, and Transformer-based forecasting baselines. Prediction error is evaluated by RMSE, MAE, and residual variance. Warning performance is measured by recall, false warning rate, and average lead time. The final metric combines prediction accuracy and warning utility. The proposed model achieves RMSE of 1.36 mm, MAE of 0.91 mm, and warning recall of 93.5% on the test set.

Results and Discussion

Prediction Accuracy Under Different Monitoring Sections

Figure 3 shows the prediction accuracy of different tunnel sections. Figure 3(a) shows the RMSE. The proposed model achieved 1.36 mm, which is better than the standard Kalman filter (1.65 mm), SVR (1.58 mm), LSTM (1.54 mm), and GRU (1.49 mm) [31]. Figure 3(b) shows the MAE and the same trend; the proposed model reduced the average error to 0.91 mm. As shown in Figure 3(c), the predicted trajectory does not exhibit the delayed

https://doi.org/10.64972/jaat.2023v1.293p11e:148-159

response of LSTM [32] and is close to the trajectory of the improved Kalman model with acceleration during the excavation process.

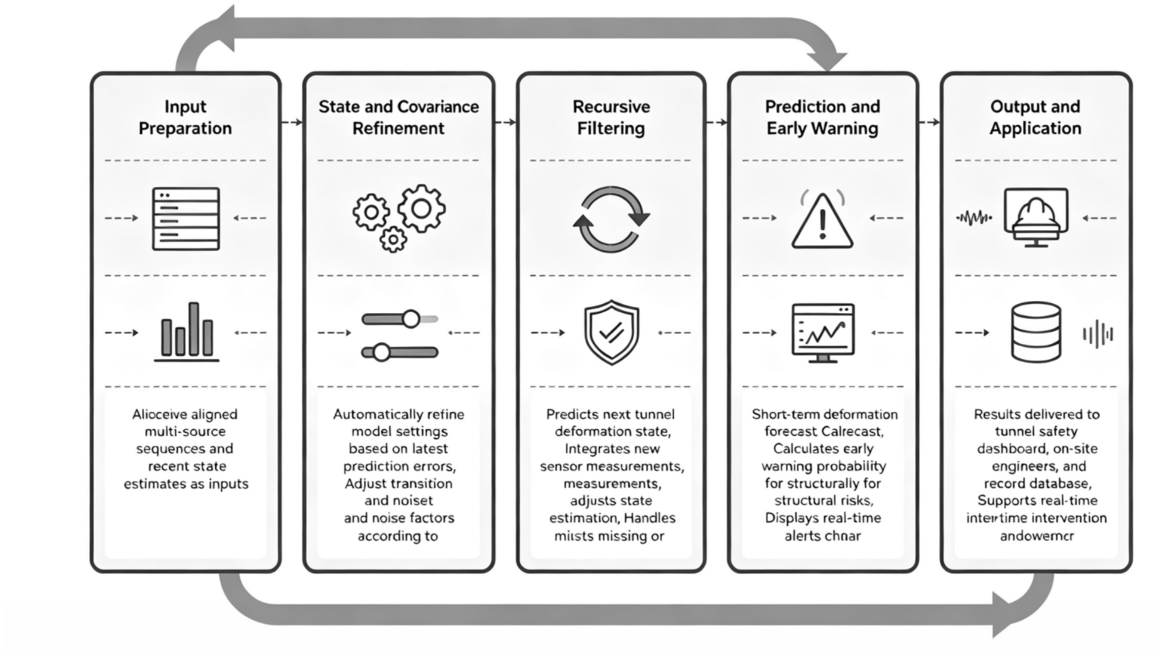

Figure 2. Adaptive state-space Kalman prediction workflow for tunnel deformation

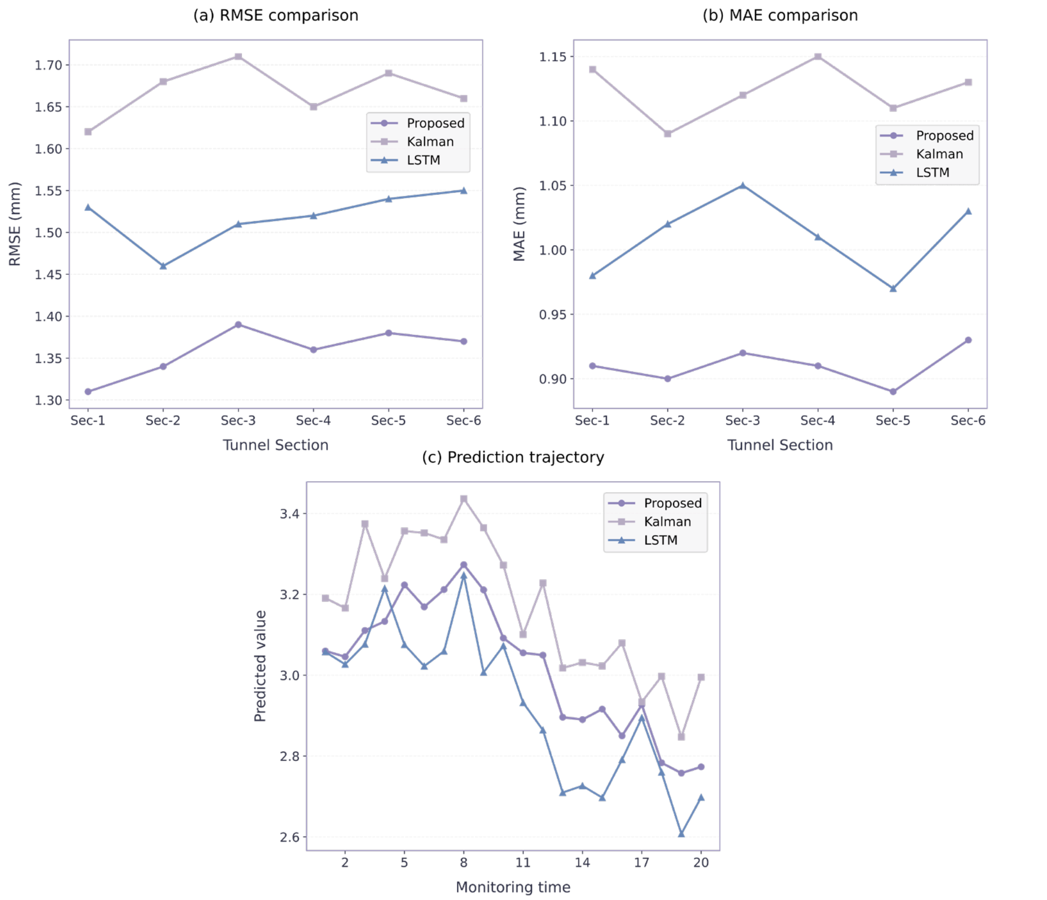

Figure 3. Prediction accuracy under multiple tunnel sections. (a) RMSE comparison. (b) MAE comparison. (c) Prediction trajectory comparison.

Figure 4 shows the residual behavior during the construction phase. As shown in Figure 4(a), the residuals during the excavation phase are larger due to the accelerated deformation in the earlier stages. The residual plot after the installation of the support is shown in Figure 4(b). The proposed model corrected the state transition faster than ARIMA and SVR. Figure 4(c) represents the steady-state operation phase, with a residual variance of 0.42 mm². Therefore, both of these improve the steady-state accuracy and the filter response speed [33].

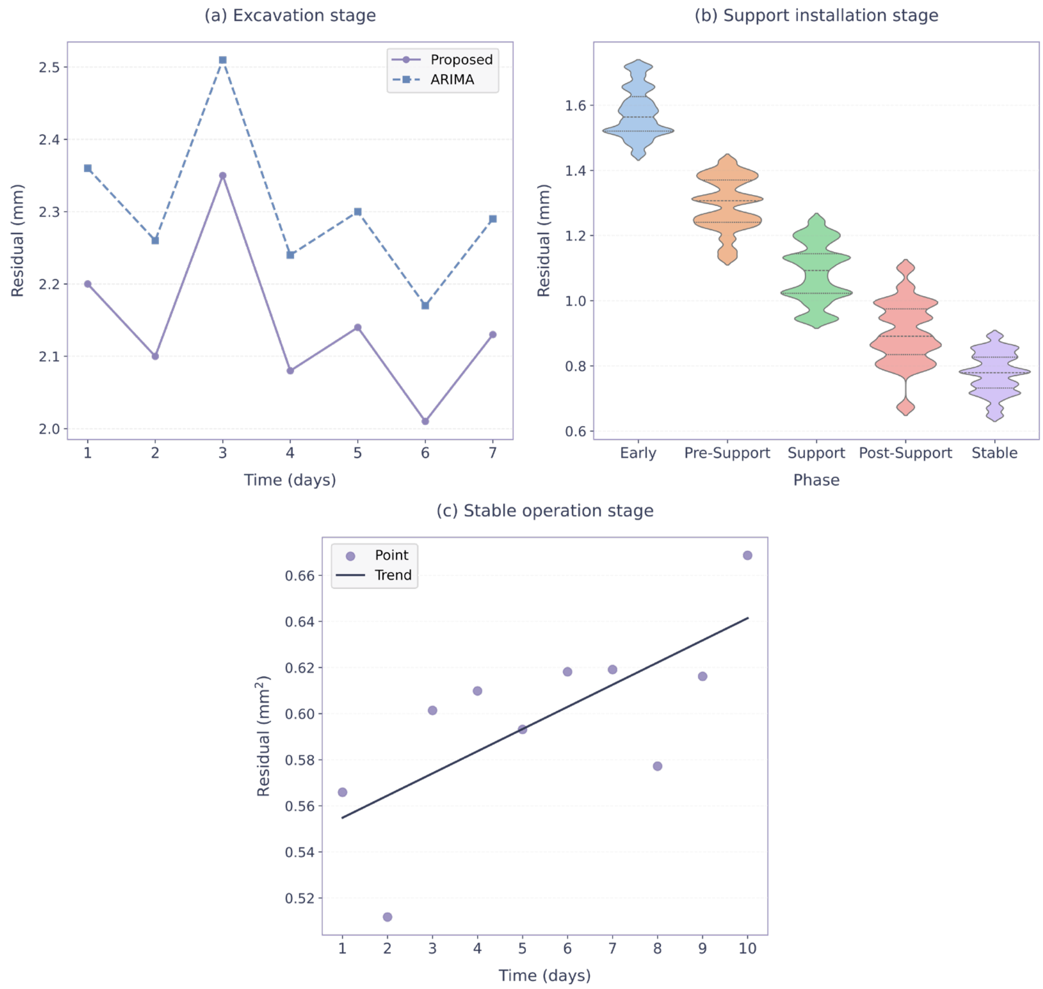

Figure 4. Residual behavior under construction stages. (a) Excavation stage. (b) Support installation stage. (c) Stable operation stage.

Robustness Under Sensor Uncertainty

In Figure 5(a), the missing data rate ranges from 5% to 30%. In the case of 20% missing observations, the root mean square error (RMSE) of the proposed model is 1.61 mm; LSTM and the standard Kalman filter increase to 2.08 mm and 2.21 mm, respectively [34]. Figure 5(b) depicts the observation noise. When the Gaussian noise reaches 10%, the residual amplification reduction of refined covariance update compared to fixed covariance filtering is 15.6%. The delayed sensor response is shown in Figure 5(c). Under the observation delay of two-time intervals, the model still maintains an alarm recall rate of over 90%.

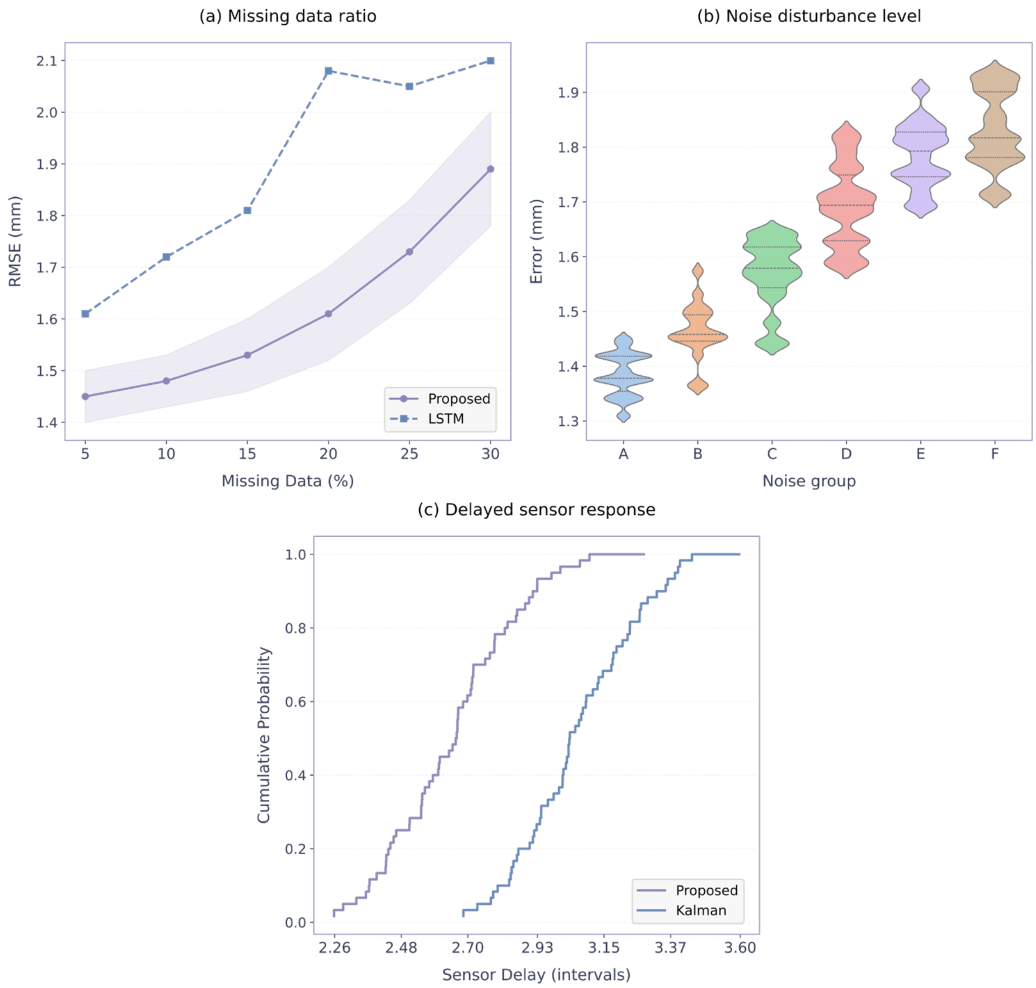

Figure 5. Robustness under uncertain monitoring data. (a) Missing data ratio. (b) Noise disturbance level. (c) Delayed sensor response.

Figure 6 shows the visualization of covariance adaptation. As shown in Figure 6(a), as the support stabilizes, the noise generated during the excavation process gradually decreases. As shown in Figure 6(b), when the sensor's reliability is low, the observation noise will also be higher. The state estimation variance in Figure 6(c) is smoother than that of the standard Kalman filter. Therefore, the warning decision should be based on deformation and uncertainty rather than a single point estimate [35].

Warning and Deployment Evaluation

Figure 7(a) shows the recall rate of early warning under low, medium, and high deformation risk levels. The recall rate of the proposed model is 93.5%, higher than that of the standard Kalman filter (87.9%) and LSTM (89.6%) [36]. Figure 7(b) shows the early warning time. The average lead time before the threshold is exceeded is 4.8 monitoring intervals. According to the inference time shown in Figure 7(c), the model's speed at each monitoring point is 2.7 milliseconds, which is below the deep sequence baseline, making it suitable for online deployment.

https://doi.org/10.64972/jaat.2023v1.293p11e:148-159

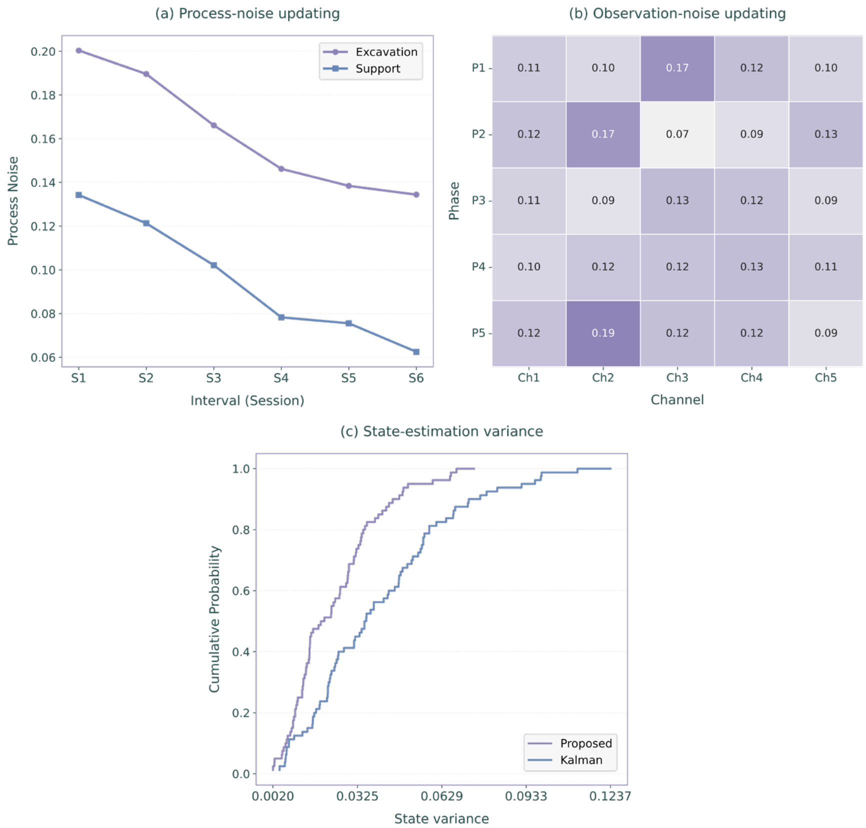

Figure 6. Covariance adaptation effect. (a) Process-noise updating. (b) Observation-noise updating. (c) State-estimation variance.

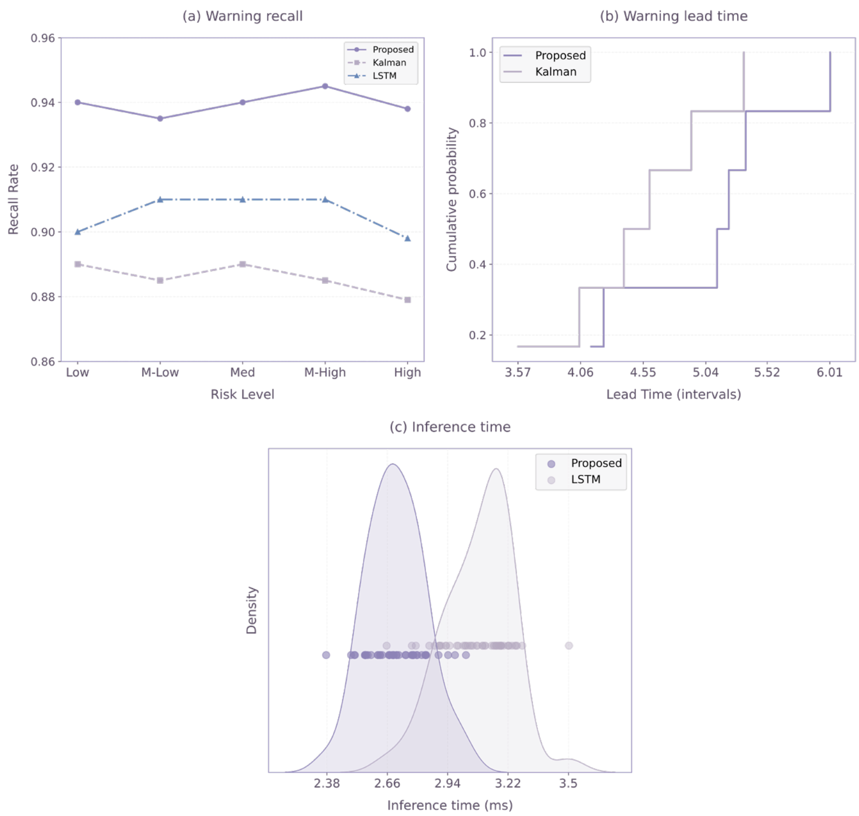

Figure 7. Warning and deployment performance. (a) Warning recall. (b) Warning lead time. (c) Inference time.

Ablation analysis verified the contribution of state space refinement. In the absence of transition refinement, the root mean square error (RMSE) is 1.36 mm, while with transition refinement, the RMSE is 1.52 mm. Due to the disabling of the adaptability of observation covariance, the false alarm rate will increase from 5.8% to 8.4%. In the presence of mining disturbances, removing the residual-guided process covariance will reduce performance and decrease the alarm recall rate by 3.1 percentage points [37]. The above results indicate that the model is one that performs residual-guided phased tunnel deformation adaptation, rather than a conventional Kalman filter with optimized parameters. The deep sequence baseline is still suitable for studying nonlinear trends, but observing changes during sparse and construction phases will increase their errors [38]. By using an improved Kalman filter, it is possible to simultaneously observe deformation speed, acceleration, covariance increase, and early warning probability [39]. The research on Bayesian convergence prediction has also expanded the application range of uncertainty-aware deformation prediction in tunnel engineering [40].

Conclusion

A paper proposes an adaptive state-space Kalman filter model based on monitoring sensor data sequences for predicting tunnel deformation. This technology first constructs a compact deformation state using settlement, convergence, velocity, acceleration, pressure correction, and residual trends. Then, based on the most recent predicted residuals, the transition matrix and covariance matrix are refined. Enhance the representation capability of the Kalman filter in uncertain monitoring, excavation disturbances, and stable support.

Experimental results show that the proposed model's prediction error is smaller than that of ARIMA, SVR, random forest, standard Kalman filter, LSTM, GRU, and the baseline conversion. In addition, it exhibits excellent robustness to missing measurements, noise monitoring, and sensor response delays. The alert probability output is suitable for real-time tunnel monitoring systems because it can improve early warning recall rates and reduce inference delays with a low false alarm rate.

In future research, a 3D tunnel scanning framework, distributed fiber optic sensing, geological prior constraints, and online parameter adaptation will be added to the system. To improve the cross-section profile, construction schedules and numerical simulation results can be added to the model. The hardware-level deployment of the edge monitoring gateway will ensure the safety of tunnel construction and operation.

Author Contributions

Hamdan Al-Suwaidi contributes to conceptualization, methodology, software, validation, analysis, investigation, data collection, draft preparation, manuscript editing, visualization, supervision, project administration, and funding acquisition. Zainab Al-Zaabi, Amal Al-Hashimi and Mishaala Al-Tunaiji contribute to validation, analysis, investigation, data collection, draft preparation. All authors have read and agreed with the manuscript before its submission and publication.

Funding

This research received no specific financial support from any funding agency.

Institutional Review Board Statement

Not applicable.

References

[1] Sun, H., Liu, S., Zhong, R., & Du, L. (2020). Cross-section deformation analysis and visualization of shield tunnel based on mobile tunnel monitoring system. Sensors, 20(4), 1006. https://doi.org/10.3390/s20041006

[2] Sun, F., Zheng, H., & Li, C. (2021). Research on prediction method of section convergence and deformation of shield tunnel in operation period based on deep learning. Vibroengineering Procedia, 39, 139-145. https://doi.org/10.21595/vp.2021.22224

[3] Cao, Y., Zhou, X., & Yan, K. (2021). Deep learning neural network model for tunnel ground surface settlement prediction based on sensor data. Mathematical Problems in Engineering, 2021, 1-14. https://doi.org/10.1155/2021/9488892

[4] Li, B., Chen, Z., & Liu, Z. (2020). Foundation settlement prediction of immersed tunnel based on monitoring data. IOP Conference Series: Materials Science and Engineering, 780(7), 072028. https://doi.org/10.1088/1757-899x/780/7/072028
[5] Mahmoodzadeh, A., Mohammadi, M., Ibrahim, H. H., Ahmed Rashid, T., Aldalwie, A. H. M., Ali, H. F. H., et al. (2021). Tunnel geomechanical parameters prediction using Gaussian process regression. Machine Learning with Applications, 3, 100020. https://doi.org/10.1016/j.mlwa.2021.100020
[6] Chen, R., Zhang, P., Wu, H., Wang, Z., & Zhong, Z. (2019). Prediction of shield tunneling-induced ground settlement using machine learning techniques. Frontiers of Structural and Civil Engineering, 13(6), 1363-1378. https://doi.org/10.1007/s11709-019-0561-3
[7] Liu, D. X., & Zhou, Y. (2020). A prediction method of ground deformation in subway tunnel construction based on Gaussian process regression. 2020 IEEE International Conference on Industrial Application of Artificial Intelligence, 1-6. https://doi.org/10.1109/iaai51705.2020.9332896
[8] Li, Z., Luan, Y., Liang, Y., & Ji, Z. (2021). Research on prediction of metro surface deformation based on ensemble Kalman Filter. IOP Conference Series: Earth and Environmental Science, 632(2), 022047. https://doi.org/10.1088/1755-1315/632/2/022047
[9] Liu, H., & Wu, W. (2021). Analysis on construction deformation characteristics of Da-Puling tunnel by monitoring measurement. IOP Conference Series: Earth and Environmental Science, 669(1), 012019. https://doi.org/10.1088/1755-1315/669/1/012019
[10] Yang, H., & Xu, X. (2021). Structure monitoring and deformation analysis of tunnel structure. Composite Structures, 276, 114565. https://doi.org/10.1016/j.compstruct.2021.114565
[11] Feng, H., Lu, T., Wang, S., Zhang, X., Luo, D., Wang, Y., et al. (2021). Monitoring techniques for settlement deformation of riverbed on shield tunnel crossing river. 2021 4th International Symposium on Traffic Transportation and Civil Architecture, 505-510. https://doi.org/10.1109/isttca53489.2021.9654731
[12] Liu, C., Wang, Z., & Jiang, Y. (2022). Settlement prediction of double line shield tunnel in upper soft and lower hard stratas. Soil Mechanics and Foundation Engineering, 59(4), 385-393. https://doi.org/10.1007/s11204-022-09826-3
[13] Hussaine, S. M., & Mu, L. (2022). Intelligent prediction of maximum ground settlement induced by EPB shield tunneling using automated machine learning techniques. Mathematics, 10(24), 4637. https://doi.org/10.3390/math10244637
[14] Kuang, G., Li, B., Mo, S., Hu, X., & Li, L. (2022). Review on machine learning-based defect detection of shield tunnel lining. Periodica Polytechnica Civil Engineering. https://doi.org/10.3311/ppci.19859
[15] Li, J., Gao, F., Lu, J., & Tao, T. (2019). Deformation monitoring and prediction for residential areas in the Panji mining area based on an InSAR time series analysis and the GM-SVR model. Open Geosciences, 11(1), 738-749. https://doi.org/10.1515/geo-2019-0058
[16] Li, D., & Wang, Y. (2020). Parameter identification of a differentiable Bouc-Wen model using constrained extended Kalman filter. Structural Health Monitoring, 20(1), 360-378. https://doi.org/10.1177/1475921720929434
[17] Li, D., & Wang, Y. (2021). Constrained unscented Kalman filter for parameter identification of structural systems. Structural Control and Health Monitoring, 29(4). https://doi.org/10.1002/stc.2908
[18] Tamuly, P., Chakraborty, A., & Das, S. (2021). Nonlinear finite element model updating using constrained unscented Kalman filter for condition assessment of reinforced concrete structures. Journal of Civil Structural Health Monitoring, 11(4), 1137-1154. https://doi.org/10.1007/s13349-021-00496-7
[19] Macchiarulo, V., Milillo, P., Blenkinsopp, C., & Giardina, G. (2022). Monitoring deformations of infrastructure networks: A fully automated GIS integration and analysis of InSAR time-series. Structural Health Monitoring, 21(4), 1849-1878. https://doi.org/10.1177/14759217211045912
[20] Amer, A., & Kopsaftopoulos, F. P. (2021). Statistical guided-waves-based structural health monitoring via stochastic non-parametric time series models. Structural Health Monitoring, 21(3), 1139-1166. https://doi.org/10.1177/14759217211024527
[21] Jeong, J., & Jo, H. (2021). Real-time generic target tracking for structural displacement monitoring under environmental uncertainties via deep learning. Structural Control and Health Monitoring, 29(3). https://doi.org/10.1002/stc.2902
[22] Hajializadeh, D. (2022). Deep learning-based indirect bridge damage identification system. Structural Health Monitoring, 22(2), 897-912. https://doi.org/10.1177/14759217221087147

[23] Ghyabi, M., Nemati, H., & Dehghan-Niri, E. (2021). A simplified framework for prediction of sensor network coverage in real-time structural health monitoring of plate-like structures. Structural Health Monitoring, 21(4), 1379-1395. https://doi.org/10.1177/14759217211033217

[24] Yuan, C., Wang, S., Qi, Y., & Kong, Q. (2021). Automated structural bolt looseness detection using deep learning-based prediction model. Structural Control and Health Monitoring, 29(3). https://doi.org/10.1002/stc.2899

[25] Lu, F., & Zeng, H. (2020). Application of Kalman Filter model in the landslide deformation forecast. Scientific Reports, 10(1), 1028. https://doi.org/10.1038/s41598-020-57881-3

[26] Peksa, J. (2020). Prediction framework with Kalman Filter algorithm. Information, 11(7), 358. https://doi.org/10.3390/info11070358

[27] Jung, S., Schlangen, I., & Charlish, A. (2020). Time-dependent state prediction for the Kalman Filter based on recurrent neural networks. 2020 IEEE 23rd International Conference on Information Fusion, 1-7. https://doi.org/10.23919/fusion45008.2020.9190484

[28] Li, G., Niu, D., & Song, E. (2020). A multiple-model state estimator based on the unscented Kalman Filter. 2020 39th Chinese Control Conference, 3011-3016. https://doi.org/10.23919/ccc50068.2020.9189548

[29] Madhukar, P. S., & Prasad, L. (2020). State estimation using extended Kalman Filter and unscented Kalman Filter. 2020 International Conference on Emerging Trends in Communication, Control and Computing, 1-4. https://doi.org/10.1109/iconc345789.2020.9117536

[30] M., S., B., R., & V., P. (2021). Uncertainty quantification in full-field displacement and strain responses of materials using Kalman Filter. Materials Today Communications, 26, 101875. https://doi.org/10.1016/j.mtcomm.2020.101875

[31] Zhou, H., Zhang, S., Peng, J., Zhang, S., Li, J., Xiong, H., et al. (2021). Informer: Beyond efficient Transformer for long sequence time-series forecasting. Proceedings of the AAAI Conference on Artificial Intelligence, 35(12), 11106-11115. https://doi.org/10.1609/aaai.v35i12.17325

[32] Lim, B., Arik, S. O., Loeff, N., & Pfister, T. (2021). Temporal Fusion Transformers for interpretable multi-horizon time series forecasting. International Journal of Forecasting, 37(4), 1748-1764. https://doi.org/10.1016/j.ijforecast.2021.03.012

[33] Benidis, K., Rangapuram, S. S., Flunkert, V., Wang, Y., Maddix, D., Turkmen, C., et al. (2022). Deep learning for time series forecasting: Tutorial and literature survey. ACM Computing Surveys, 55(6), 1-36. https://doi.org/10.1145/3533382

[34] Torres, J. F., Hadjout, D., Sebaa, A., Martinez-Alvarez, F., & Troncoso, A. (2021). Deep learning for time series forecasting: A survey. Big Data, 9(1), 3-21. https://doi.org/10.1089/big.2020.0159

[35] Phan, T. T. H., & Nguyen, X. H. (2020). Combining statistical machine learning models with ARIMA for water level forecasting: The case of the red river. Advances in Water Resources, 142, 103656. https://doi.org/10.1016/j.advwatres.2020.103656

[36] Wang, Q., & Wang, S. (2020). Machine learning-based water level prediction in Lake Erie. Water, 12(10), 2654. https://doi.org/10.3390/w12102654

[37] Xu, M., Chen, J., & Yang, H. (2021). Time series of landslide displacement prediction based on VMD-LSTM. 2021 International Conference on Neuromorphic Computing, 215-220. https://doi.org/10.1109/icnc52316.2021.9608039

[38] Pei, H., Meng, F., & Wang, L. (2021). Uncertainty elevation of landslide displacement prediction based on LSTM and Mixture Density Network. IOP Conference Series: Earth and Environmental Science, 861(4), 042047. https://doi.org/10.1088/1755-1315/861/4/042047

[39] Xu, C., Huang, K., Wei, C., & Lin, Y. (2022). Landslide displacement prediction based on variational mode decomposition and LSTM. 2022 20th International Conference on Optical Communications and Networks, 1-3. https://doi.org/10.1109/icocn55511.2022.9900981

[40] Chang, X., Wang, H., Zhang, Y., Wang, F., & Li, Z. (2022). Bayesian prediction of tunnel convergence combining empirical model and relevance vector machine. Measurement, 188, 110621. https://doi.org/10.1016/j.measurement.2021.110621